ADVANCED FUNCTIONAL MATERIALS

www.afm-journal.de

PEI金属化优点：
机械强度、生物相容性、
耐化学性、耐高温

实现方法：
嵌入银纳米线、
分解金属有机化合物、
活化金属钯

A Rapid Photopatterning Method for Selective Plating of 2D and 3D Microcircuitry on Polyetherimide

Jose Marques-Hueso, Thomas D. A. Jones, David E. Watson, Assel Ryspayeva, Mohammadreza Nekouie Esfahani, Matthew P. Shuttleworth, Russell A. Harris, Robert W. Kay, and Marc P. Y. Desmulliez*

AgCl光敏材料，在聚合物表面析出Ag

金属微型管道

聚醚酰亚胺，3D打印材料

该研究基础：
AgCl比其他
反应物更快

PEI相当于底座

In this work, a method for the rapid synthesis of metallic microtracks on polyetherimide is presented. The method relies on the photosynthesis of silver nanoparticles on the surface of the polymer substrates from photosensitive silver chloride (AgCl), which is synthesized directly on the polyetherimide surface. The study reveals that the use of AgCl as a photosensitive intermediate accelerates the reactions leading to the formation of silver nanoparticles by up to two orders of magnitude faster than other photodecomposition schemes. The patterning can be conducted under blue light, with notable advantages over UV exposure. Polymers of significant interest to the microelectronics and 3D printing industries can be directly patterned by light using this photography-inspired technique at throughputs high enough to be commercially advantageous. Light exposures as short as a few seconds are sufficient to allow the direct metallization of the illuminated polyetherimide surface. The results show that the silver required for the seed layer is minimal, and the later copper electroless plating results in the selective growth of conductive tracks for circuitry on the light-patterned areas, both on flexible films and 3D printed surfaces.

只需几秒钟，便可在PEI表面聚合出Ag

种层需要很少Ag，后面的铜化学特性导致
其在导电轨道和特定图案上选择性生长

1. Introduction

柔性基表面的导电轨道可实现不同图案的绘制　电镀

Micropatterning of conductive tracks on flexible substrates and contoured surfaces enables a multitude of novel packaging solutions.[1] This is an area of major research interest, with new additive techniques continuously being proposed, such as ink-jet printing,[2] plating of modified surfaces,[3] and the direct metallization[4] of modified photoresists,[5] which has the advantage that it can be directly patterned by UV photolithography[6] without vacuum process steps for the metal deposition.

可变光刻胶的直接金属化

有真空步骤

相较于光刻法金属沉积，更有优势

The metallization of polyimides has received particular attention, due to their mechanical strength, biocompatibility, chemical resistance, and ability to withstand high temperatures. Different approaches have been followed to achieve this metallization, such as embedding silver nanowires,[7] decomposing metal–organic compounds[8] or the activation of a palladium seed layer for future plating.[9]

One proposed methodology for the fabrication of metallic tracks on polyimides is surface modification by ion exchange and subsequent plating.[10] This method has the advantage of avoiding any vacuum processing steps. Moreover, the organometallic bonds can be selectively broken by irradiation, enabling direct light patterning. Finally, the use of a photoresist acting as a mold for electroplating can be removed from the manufacturing process. The nanoparticles (NPs) resulting from the photoreduction of the free metallic ions can then be used as seeds for subsequent plating. This also permits patterning by direct laser writing,[11] which could accommodate the selective plating of contoured, 3D surfaces.

聚酰亚胺PI

表面改性

离子交换和分层电镀

有机金属件被选择性破坏

直接光图案化

光刻胶

纳米粒子

游离金属离子光还原产生的纳米颗粒，可用作后续电镀种层

可以在3D轮廓表面直接用激光进行刻画

This manufacturing process has a plethora of advantages, but its industrial implementation has been held back as the photopatterning stage has been too slow to be implemented for mass production. Moreover, the exposure energy must be limited in order to avoid damage to the polymeric substrate.[12] These limitations have triggered a search for new processes in order to obtain faster nanoparticle formation.

上述技术有诸多优点，
工业实施却处于滞后阶段。
缺点：光刻图阶段过慢
曝光能量需被严格控制
（防止破坏聚合物基座）

使用温和还原剂

One approach has been to use assisted photoreduction of the metallic ions with a mild reducing agent[12] such as methoxy poly(ethylene glycol) (MPEG), at the expense of long exposure times of over one hour. The photopatterning has also been replaced by selective surface modification using directed ink-jet droplets;[13] this however places limitations on manufacturing flexibility. Electric fields have also been utilized to assist the metallization process.[14] Selective site chemical reduction by dimethylamine borane solution[15] has shown a fast reduction,

甲氧基聚（乙二醇）（MPEG）

金属化过程中，也可外加电场

二甲胺硼烷溶液

加入合适的溶解液，加快还原速度

Dr. J. Marques-Hueso, Dr. T. D. A. Jones, Dr. D. E. Watson, Dr. A. Ryspayeva, Prof. M. P. Y. Desmulliez
School of Engineering & Physical Sciences
Nature Inspired Manufacturing Centre (NIMC)
Heriot-Watt University
Edinburgh EH14 4AS, Scotland, UK
E-mail: J.Marques@hw.ac.uk

Dr. M. Nekouie Esfahani, M. P. Shuttleworth, Prof. R. A. Harris, Dr. R. W. Kay
Future Manufacturing Processes Research Group – School of Mechanical Engineering
University of Leeds
LS2 9JT, UK

The ORCID identification number(s) for the author(s) of this article can be found under https://doi.org/10.1002/adfm.201704451.

DOI: 10.1002/adfm.201704451

FDM:fused deposition modeling(熔融沉积成型工艺)

缺点：引入了基于抗蚀剂的处理步骤

but introduces new resist-based processing steps. A recently proposed method to reduce the damage to the substrate relies on the repetition of an iterative sequence of ion-exchange/reduction/regeneration using up to 23 cycles,[16] making the method time consuming. In light of this, a solution for the fast photopatterning of polyimides for microcircuitry generation has yet to be found.

PEI有着和PI类似的物理化学性质，但PEI可用于3D打印

Silver ion exchange and nanoparticle synthesis by chemical reduction has been demonstrated for polyetherimide (PEI).[17] PEI has the same excellent properties as PI, and has many applications in medical, electronic/electrical, microwave, automotive, and aerospace industries. Compared to polyimide, it has the advantage that it can be 3D printed, with fused deposition modeling (FDM) filaments being commercialized under the names of ULTEM 9085 and 1010. This polymer is printed via FDM at a high temperature of 315–400 °C, which is ≈100 °C higher than other commonly used polymers for FDM. For this reason and its good flame retardant nature, it is reserved for the manufacture of high value objects in sectors such as aerospace. Moreover, it is USP Class VI compliant, which enables its use in medical devices.

PEI使用FDM工艺时温度约315-400度，比其他聚合物高100度

PEI还可用于航空领域，以及医疗器械领域

The possibility to create customized circuitry on the surface of 3D plastic substrates enables new applications, which is highlighted in the success of the laser direct structuring method used to create circuitry on 3D surfaces.[18] In this method, a metallic precursor is sprayed onto the surface of a sample before laser structuring. This is used to create molded interconnect devices, which are commonly used for cell-phone antennas, automotive wiring components or in medical devices.

定制电路

金属前体

模塑互联设备

In this work, we present a method that enables the rapid photopatterning of polyetherimide for later selective plating. The method involves the production of photosensitive AgCl on the surface of the polymer. Conductive tracks on flexible substrates are obtained. The method is also applied with similar results to PEI filaments used in FDM for 3D printing. This work is relevant to the microelectronics industry as well as the 3D printing manufacturing sector.

2. Results and Discussion

The process to obtain the metallic tracks is shown in **Figure 1**a. After degreasing, the samples were immersed in a 15 M KOH bath at 50 °C. The high alkaline conditions were required to modify the surface of the resistant PEI. Under these conditions, the imide ring (O=C−N−C=O) opens and becomes an amide (N−C=O). The remaining part of the ring presents an open bond that allows the attachment of a potassium ion. In a later immersion in silver nitrate solution, the silver ions replace the potassium by ion exchange in a well-known reaction,[19] which results in the production of silver polyamate, as shown in Figure 1b. The process can be monitored by infrared spectroscopy. Figure 1c shows the Fourier transform infrared (FTIR) spectra of ULTEM 9085 samples at different stages of the process. The absorption lines of an untreated sample are displayed in black. Characteristic lines for imide group appear clearly at 1370, 1710, and 1780 cm^{-1}. These correspond with the C−N−C, C=O symmetric, and the C=O double bond asymmetric stretches of the imide ring, respectively. After treatment

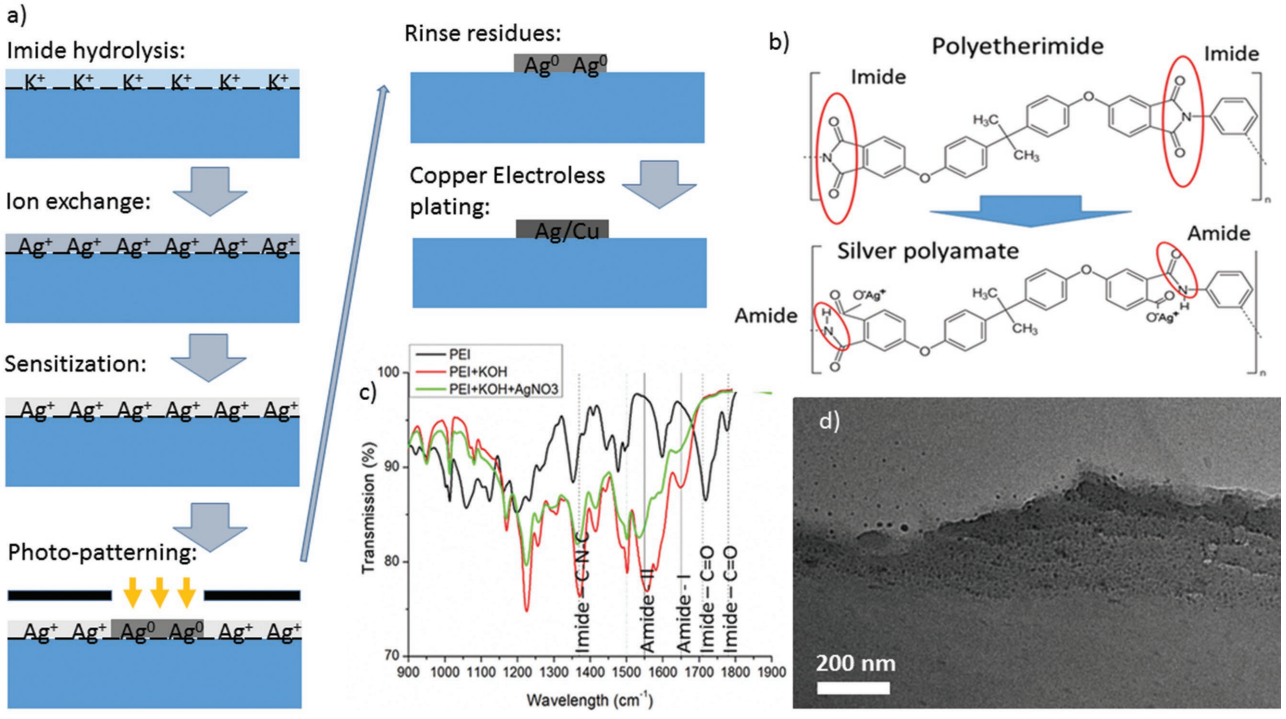

Figure 1. a) Process to achieve the metallization of polyimide and polyetherimide. The sensitization step is crucial to achieve a fast process. b) Hydrolysis breaking of the imide ring. Potassium ion was replaced by silver using ion exchange, which produced silver polyamate. c) FTIR of the PEI at different stages of the process. d) TEM cross-section of ULTEM 9085 treated sample revealing the NPs on its surface.

with KOH (red line), these peaks are attenuated, which denotes the opening of the imide ring. New peaks appear, namely the amide I and II vibrations, at 1650 and 1550 cm^{-1}, respectively. After immersion in silver nitrate solution, the silver atom replaces the potassium atom, which does not translate in any major change of the FTIR spectrum (green line). Figure 1d shows the cross-section of an ULTEM 9085 sample after silver treatment and reduction as described previously. The silver nanoparticles have been synthesized as a few hundred nanometers thick layer on the surface of the sample.

Light exposure under the correct conditions induces the formation of nanoparticles as a result of the photodecomposition of silver polyamate and therefore the reduction of the silver ions (Ag^+) to the metallic state (Ag^0). Selective etching can remove the silver compound of the unexposed areas without significantly affecting the nanoparticles. The nanoparticles can then be used as a seed layer for electroless copper plating. Two approaches have been applied in order to speed up the nanoparticle formation: sensitization and exposure parameter optimization.

2.1. Sensitization

The first approach to accelerate the production of silver nanoparticles is to modify the photosensitive compound. Silver polyamate photodecomposes slowly.[11] For this reason, the process can be accelerated through the use of an intermediate with a higher photosensitivity. AgCl has been chosen here due to its high photosensitivity[20] and its ease of synthesis. After the immersion in silver nitrate and a deionized (DI) water rinse, a short immersion in 0.01 M KCl in ethanol: water (3:1) was performed. This results in the rapid amalgamation of the chloride and silver ions in a well-known reaction, where the highly insoluble halide salt AgCl is precipitated on the surface of the film, as the following reaction

$$Ag^+ + KCl \rightarrow K^+ + AgCl(s) \quad (1)$$

Light exposure can trigger the photocatalysis of the white component AgCl into metallic silver and chlorine gas

$$2AgCl(s) \rightarrow 2Ag(s) + Cl_2(g) \quad (2)$$

Figure 2 shows the photopatterning of ULTEM 1000B under illumination from a UV mask aligner (i-line from mercury lamp at 365 nm) and a chromium mask. When KCl was used, very short exposures of 3 s at 11 mW cm^{-2} achieved the patterning of the sample. The optical contrast increased for higher exposure times. In the presence of KCl it took only 30 s to achieve a comparable optical contrast to samples exposed for 1 h without KCl. This represents a time difference between the processes of two orders of magnitude. The photodecomposition of AgCl resulted in a red color, as other authors have also observed.[21] This color could be due to the possibility of having metallic Ag on AgCl,[21] with the refractive index of AgCl being ≈2 in the visible range.[22] The proximity of this high refractive index material to the silver nanoparticles could redshift the plasmon resonance. The visible color of NPs is also influenced

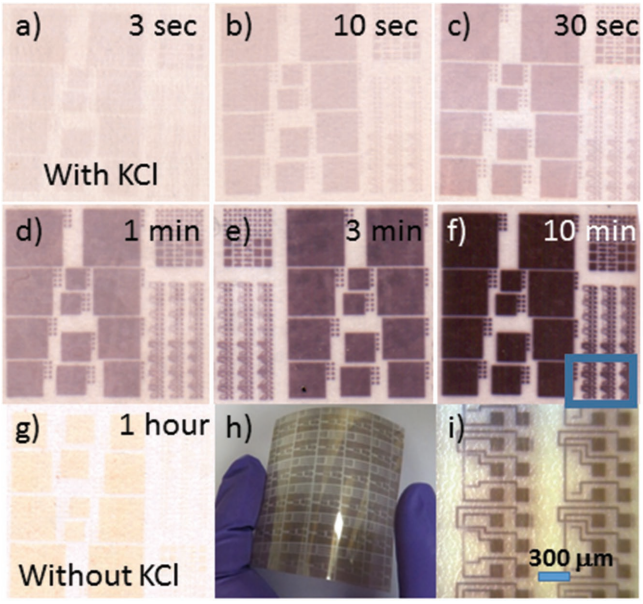

Figure 2. a–f) Photopatterned 1000B ULTEM polyetherimide samples at different exposure times when sensitized with KCl. g) Sample without KCl treatment, showing a longer required patterning time. h) 7 × 7 cm^2 patterned flexible sample. i) 18 µm wide tracks (detail from (f)).

by particle size[23] or possible agglomerates.[24] If the NPs are large, ultimately the samples would appear silver-plated, as shown later.

Two analytical techniques were applied to verify the presence of AgCl. **Figure 3**a shows the X-ray diffraction (XRD) pattern of a PEI ULTEM 1000B sample after silver treatment, immersion in KCl solution, and light exposure. The image shows a series of peaks that adjust to metallic silver (JCPDS card 00-004-0783 for fcc silver) and AgCl (JCPDS card 00-031-1238). Figure 3b shows a scanning electron microscopy (SEM) image of a KCl treated sample unexposed to light. The SEM imaging was difficult to obtain because the substrate was nonconductive and photosensitive—making it susceptible to the incoming electrons causing the unwanted release of Cl and leaving metallic Ag behind. The analysis was performed as quickly as possible to avoid excessive surface modification, although some modification is expected due to the high energy of the electrons and the photosensitive nature of AgCl. The results revealed a high content of silver (7% atomic), and lower amounts of Cl (1.6%) and K (0.9%) and, because the Cl content exceeded the K percentage, some of the chloride was likely contained as AgCl. The Ag content was much higher, which could have come from two effects. First, it is possible that some silver failed to react with Cl and some amounts of silver polyamate remained after the KCl immersion. However, Ag is known to react readily with halide ions, and it could be expected that most of the silver had reacted when exposed to Cl ions. Second, and more likely, the electron beam of the SEM reacting with the AgCl film could have released part of the Cl in gaseous form, and left behind solid metallic silver. This could explain the excess of silver when using this technique.

After the photopatterning of samples, it was necessary to remove the silver residues from the unexposed areas in order to be able to obtain selectivity when plating. Without this stage,

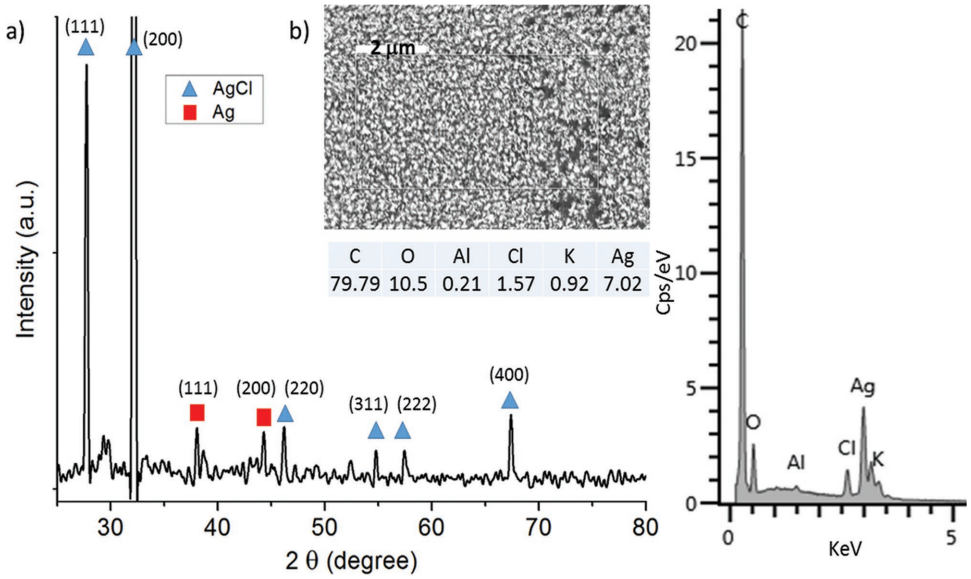

Figure 3. XRD spectra of a sample of PEI after silver treatment, KCl sensitization, and 10 min light exposure. b) SEM from a KCl treated sample, unexposed with light. The EDX analysis reveals Ag, Cl, and K content (atomic percentage).

the entire surface would become plated. The remaining AgCl was dissolved using ammonia. The ammonia tends to form diamine silver, which is a stable and soluble compound. The reaction follows the formula

$$AgCl + 2NH_3 \rightarrow \left[Ag(NH_3)_2\right]^+ + Cl^- \quad (3)$$

A diluted solution of sulfuric acid was then used to remove any possible remaining Ag^+.

Systematic experiments have shown that the most effective cleaning consists of an initial immersion in ammonia (35%, 20 s) followed by a rinse in DI water, and finally immersion in sulfuric acid (H_2SO_4, 5%, 3 min). A sample prepared following this methodology is shown in **Figure 4**. The plating process consisted of a single immersion in the copper electroless plating bath described in the Experimental Section. Plating under these parameters was selective and 18 µm wide tracks can be perfectly defined (Figure 4b). The resistance along the black arrow in Figure 4a has been measured as 40 Ω using a two-point probe station. The metallic surface was composed of small compacted Cu grains, which is an indicator of high quality and good conductivity for electroless plated copper (Figure 4c). While 18 µm is a functional size, the technique allows further miniaturization. One of the main limiting factors on the critical feature size is the arithmetic average roughness (R_a), which can be very small in the case of PEI (in our samples it was measured as R_a = 12 nm by profilometry). The feature size has been reduced to 2 µm platted lines (see Figure S1, Supporting information).

2.2. Effect of Exposure Wavelength and Dose

The patterning process can also be improved by optimizing the exposure parameters as both wavelength and power are relevant to trigger the silver photoreduction.

Figure 5 shows the optical contrast of the photopatterned ULTEM 1000B silver and KCl treated samples. Different wavelengths at the same power were used, with a low power (110 mW cm^{-2}) chosen to avoid thermal damage. There has been a trend in the literature[12,19] to use light in the UV range to achieve selective NP synthesis since UV photons carry more energy and are more easily absorbed by most materials. However, in this work, wavelengths in the range of 410–470 nm have been shown to be more effective than 375 nm. The lower efficiency at short wavelengths could be due to two reasons. The first is a possible competition between the polymer and the KCl layer for available photons. Polyetherimide is transparent in the visible spectrum, but it absorbs very strongly at wavelengths shorter than 400 nm resulting in less photons available

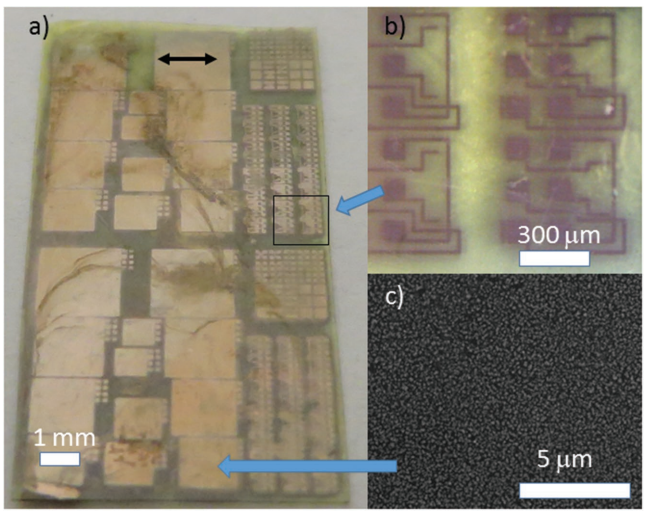

Figure 4. a) Photopatterned sample after 5 min 30 s Cu plating. b) Detail of the sample showing 18 µm tracks. c) SEM image of the surface of plated copper showing a compact surface of small grain structure.

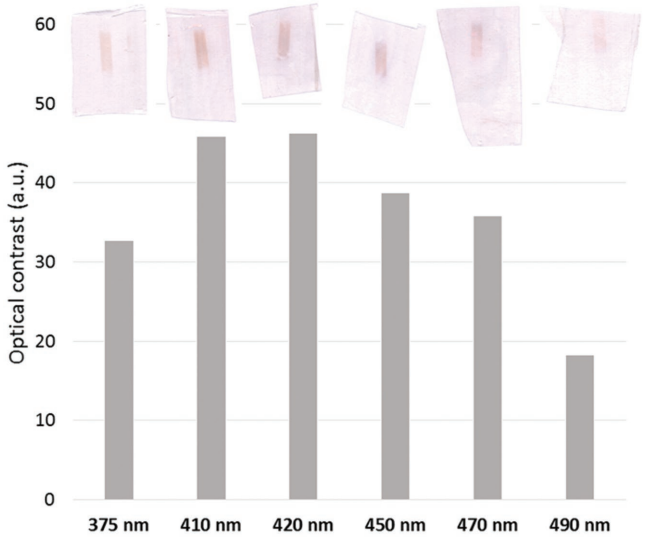

Figure 5. Optical contrast of patterns obtained at different wavelengths on ULTEM 1000B (width of patterned tracks: 1.2 mm).

to dissociate the AgCl. However, this explanation is less likely as the silver layer on top of the PEI will reflect and absorb the majority of the oncoming light, thus shielding the PEI layers underneath. The second more likely explanation is plasmonic resonance enhancement.[25] In this case, the growing metallic NP could benefit from a larger optical absorbance due to the localized surface plasmon resonance.[17] This would gather the incoming light more effectively. The plasmon resonance of silver NPs is located at the blue part of the spectrum, which would explain why blue light is more effective than UV to synthesize the NPs.

The use of blue light has important practical advantages compared to UV exposure, which include safety, costs, and easy availability of sources. It also allows for the use of higher intensities to be applied. Moreover, the use of discrete sources has the advantage over flood exposure in that it can be focused, enabling future laser patterning without the need of a photomask. Finally, blue light is less damaging to polymers than UV wavelengths.

For these reasons, a high-power blue LED was used for subsequent experiments. The peak power of 12 W cm^{-2} provided a good compromise between providing a fast patterning while avoiding unwanted thermal effects and not producing visible damage to the polymer surface. **Figure 6** shows the achieved patterning without (a) and with (b) KCl treatment. The exposure times revealed that the patterning was achieved significantly faster than with UV flood exposure. When KCl was applied, the samples exposed for 3–10 s produced an optical contrast similar to the sample exposed for 10 min without KCl treatment. Moreover, the intensity profile of the LED was a Gaussian shape with full width at half-maximum = 2.2 mm. This meant that the intensity a few millimeters away from the center was significantly smaller than at the central point (about 100 times lower just 2 mm away from the center). In light of this, the exposure time to achieve photopatterning was reduced by more than two orders of magnitude.

Figure 6c shows the absorbance of the KCl processed samples. The absorbance at wavelengths lower than 400 nm was due to the PEI polymer. While the nucleation and growth of the metallic NPs was monitored in the time span, the small difference in intensity from 3 to 10 min of exposure produced an insight into the saturation time of the reaction. A clear peak appeared at 450 nm, due to the localized surface plasmon resonance of the silver NPs. This peak exhibited a broad tail in the

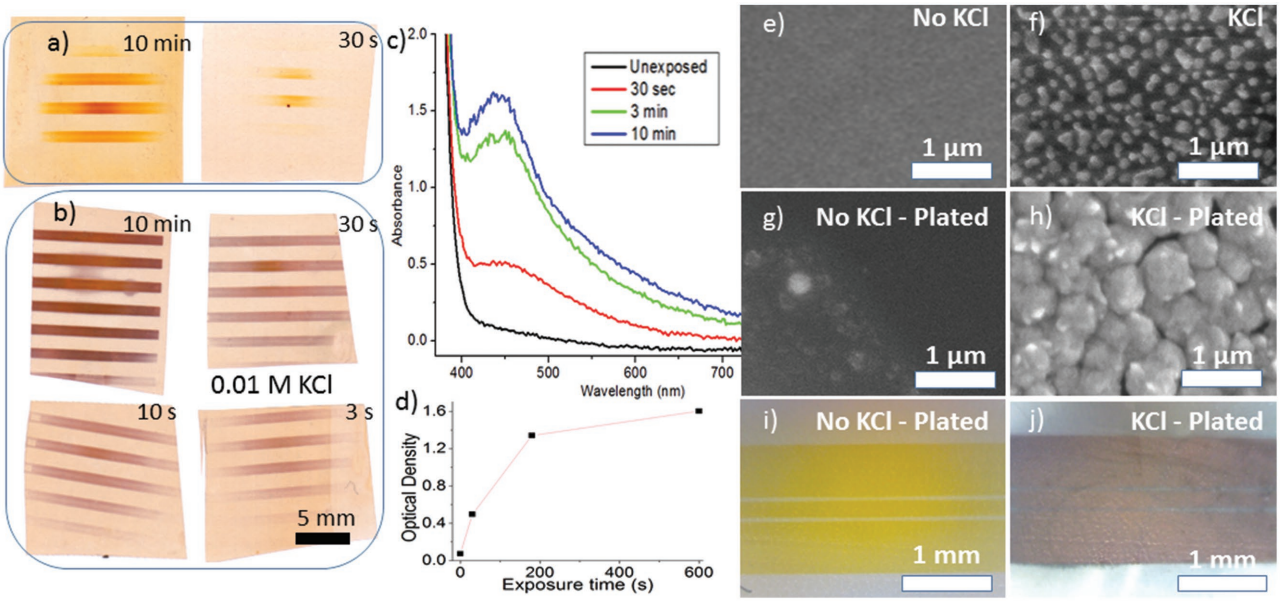

Figure 6. a) Patterning on ULTEM 1000B using 460 nm LED without KCl. b) Patterning using a 30 s immersion in KCl. c) Optical absorbance of the patterned regions for samples with KCl. d) Optical density at 450 nm. e,f) FESEM image of the surfaces for exposed samples without and with KCl treatment. g–j) Their corresponding surface after copper plating during 20 min.

entire visible spectrum, which is a common feature of samples with polydispersity of NP sizes,[26] justifying the red hue of the patterns. Figure 6d shows the optical density of the films at 450 nm, revealing saturation for 10 min exposure. The SEM analysis of the samples reveals difference between samples processed without/with the KCl treatment. For 10 min exposure, the NPs of the sample without KCl treatment are not visible by SEM, possibly due to their small size (Figure 6e). Silver nanoparticles of only a few nanometers in size are known to present a clear localized surface plasmon resonance, while their size would be too small to be observed by SEM. On the surface of the KCl treated sample (Figure 6f) large silver NPs of average size 141 nm are formed. These NPs are located in a film ≈100 nm thick (see Figure S2, Supporting Information). The formation of this layer enables activation of the surface and plating. The samples have then been washed with sulfuric acid and ammonia, and immersed in copper plating solution for 20 min. Figure 6g shows the sample without KCl treatment after the plating process highlighting that no observable growth of copper has occurred. Conversely, the sample treated with KCl presents a deposit of compact copper (Figure 6g). This film is 359 ± 45 nm thick, and its conductivity is high at (3.1 ± 1.5) × 10^7 (Ω m)$^{-1}$, which is half of bulk copper, (5.96 × 10^7 (Ω m)$^{-1}$). Optical microscopy and naked eye inspection additionally reveal that the sample treated with KCl has a compact deposit of copper after the plating (Figure 6j).

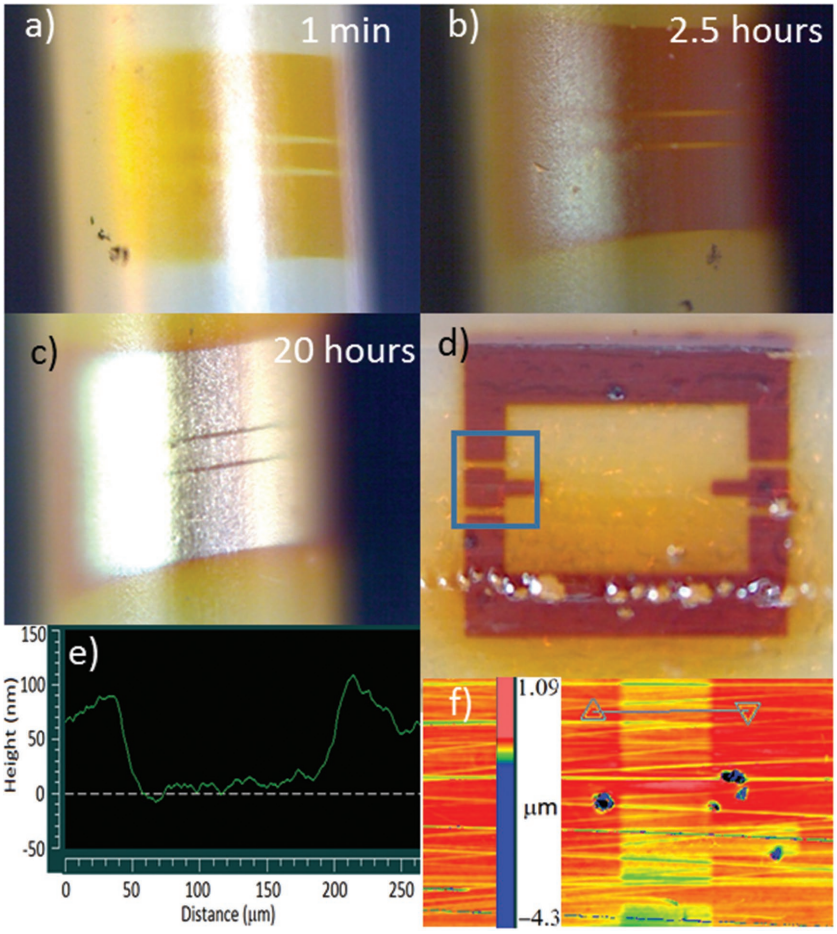

Figure 7. a–d) Polyetherimide ULTEM 9085 silver treated samples exposed at 460 nm. e–f) Profilometric measurements of (d), which was exposed for one hour.

In further experiments, the ion exchange silver treatment was also shown to work for polyetherimide ULTEM 9085, which is used in 3D printing. With low exposure times at 460 nm (12 W cm^{-2}), the exposed area became yellow (**Figure 7**a), which agrees with the color of small silver nanoparticles. After 2.5 h (Figure 7b) the color has become reddish, which could be explained by the agglomeration of silver nanoparticles, which red-shifts the plasmon resonance. Finally, at long exposure times over 20 h (Figure 7c), the sample has a metallic silver look, which occurs when the NPs coalesce into larger silver structures. The resistance of this last sample was 44 ± 0.2 Ω for an electrode distance of 0.42 mm. This resistance is very low for a sample that has not been copper electroless or electroplated, but only treated with blue light.

The long exposure time however would prevent any industrial use. Moreover, the new exposure parameters have the inconvenience of producing some surface damage during these prolonged exposures. Figure 7d shows a sample exposed for one hour. The optical profilometer measurements reveal that the substrate had recessed by 70 nm in one hour (Figure 7e,f). This result is in line with photodegradation values for polyimide Kapton 200 HN (DuPont).[27] In order to avoid this damage, it is necessary to reduce the exposure time.

A faster reaction was achieved when using the KCl treatment. **Figure 8**a,b shows two samples that were silver treated, optically exposed for one minute and electroless plated, the first without KCl treatment and the second one with. While the first sample had not modified its appearance after plating, the KCl treated sample showed a clear deposit of copper. The low definition of the boundaries was due to the use of a planar chromium mask for photoexposure on the curved surface of the plastic filament, which produced diffused light away from the contact point. However, in the central contact region it was possible to observe the two horizontal thin lines (35 μm wide) of the mask. Figure 8c shows a 3D printed sample where the treatment with KCl and later electroless plating was performed. A 310 μm wide copper track was selectively deposited with a resistance of 18 ± 0.2 Ω for an electrode distance of 3.0 mm.

3. Conclusion

A fast photopatterning method to synthesize silver nanoparticles on polyetherimide has been developed. The synthesis of AgCl as photosensitive intermediate accelerates the photoreduction and formation of nanoparticles, which can be obtained in 3 s, representing a speed by up to two orders of magnitude in

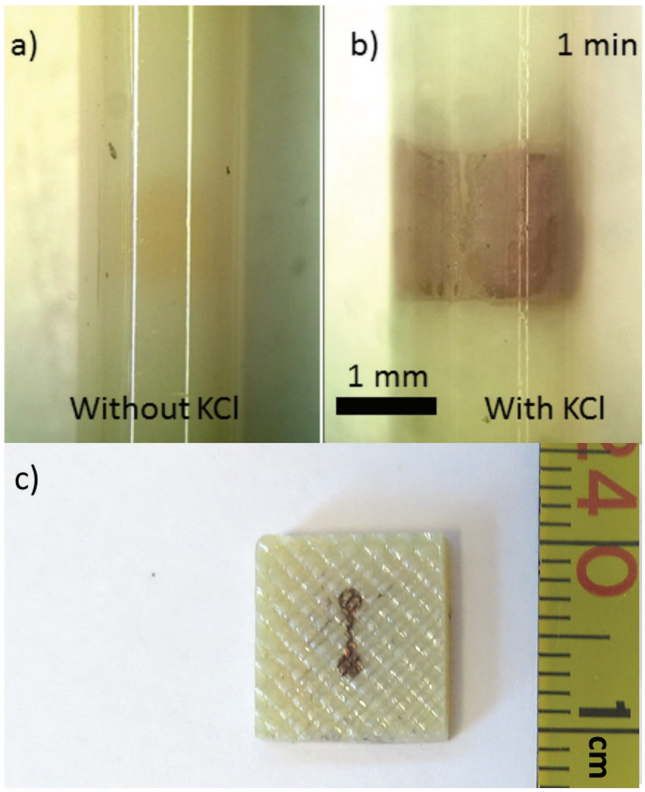

Figure 8. Polyetherimide ULTEM 9085 samples exposed at 460 nm, a) without and b) with KCl treatment, and after 20 min immersed in a copper electroless plating solution. c) 3D printed sample patterned at 460 nm with KCl treatment, and selectively copper plated.

relation to unsensitized samples. The optimization of the exposure parameters has shown that the use of blue light was more convenient and efficient than UV exposure. The light-induced synthesis of silver NPs enables the selective plating with copper of the light treated areas, obtaining conductive tracks. Tracks as small as 18 µm have been fabricated, which enables their use for microcircuitry. The method has been demonstrated to work for flexible polyetherimide films as well as for polymer material used for 3D printing.

4. Experimental Section

Polyetherimide sheets (75 µm thick grade 1000B ULTEM) were purchased from Cadillac Plastics, U.K. Polyetherimide 1.75 mm diameter filament for FDM, ULTEM 9085, was purchased from Stratasys Ltd. The remaining chemicals were obtained from Fisher Scientific, U.K.

The samples were cleaned with isopropanol for degreasing before treatment. The samples were immersed for 15 min in a heated potassium hydroxide (KOH, 15 M) solution bath at 50 °C. After rinsing with DI water and ultrasound agitation, the substrate was submerged in a 0.1 M silver nitrate ($AgNO_3$) solution for 15 min, and a new DI water rinse was performed. When the KCl treatment was applied, the samples were submerged in a 0.01 M KCl solution (ethanol:water, 3:1), for 30 s, and were then allowed to dry under ambient conditions.

Two different light sources were used for the exposure. (1) A photolithography mask aligner (11 mW cm^{-2} at 365 nm) for flood exposure, and (2) a high-power LED at 460 nm (1 W) for local exposure. A chromium mask was used for selective exposure. The removal of metallic residues after optical exposure was performed by immersing the sample in ammonia, a rinse in DI water, an immersion in diluted sulfuric acid, and finally a rinse with DI water. The optimal parameters for the flexible film ULTEM 1000B were 20 s in ammonia (35%) and 3 min in sulfuric acid (5%). Optimal parameters for the filament ULTEM 9085 were 15 s in ammonia (17%) and 20 s in sulfuric acid (5%). After this, the samples were plated in an electroless copper solution comprising of 15 g L^{-1} copper (II) sulfate pentahydrate, 20 g L^{-1} sodium hydroxide, 70 g L^{-1} sodium potassium tartrate, and 77 mL L^{-1} formaldehyde 37%. The solution was made up to the procedure outlined within[28] and the samples were immersed for a period between 20 and 30 min at 20 °C.

FTIR measurements were obtained with a Perkin-Elmer Spectrum 100 FT-IR spectrometer in attenuated total reflection (ATR) mode. SEM images were taken using a Quanta 3-D FEG from FEI Company, USA. XRD measurements were performed with a D8 Discover, from Bruker Corporation (λ = 0.15418 nm). Optical absorbance was measured using a Perkin-Elmer LAMBDA 950 UV–Vis Spectrophotometer. Polyetherimide ULTEM 9085 was 3D printed applying an extrusion temperature of 315 °C, and a bed temperature of 195 °C.

Supporting Information

Supporting Information is available from the Wiley Online Library or from the author.

Acknowledgements

The authors thank the Engineering & Physical Sciences Research Council (EPSRC) for their financial support under the grants Photobioform I (Grant Nos. EP/L022192/1 and EP/L022133/1) and Photobioform II (Grant Nos. EP/N018222/1 and EP/N018265/2). Figure 8 c) and the Toc Figure were updated on February 7, 2018, following initial publication on early view.

Conflict of Interest

The authors declare no conflict of interest.

Keywords

3D printing, circuitry, photopatterning methods, plating, polyetherimide

Received: August 5, 2017
Revised: October 11, 2017
Published online: December 15, 2017

[1] A. Nathan, A. Ahnood, M. T. Cole, S. Lee, Y. Suzuki, P. Hiralal, F. Bonaccorso, T. Hasan, L. Garcia-Gancedo, A. Dyadyusha, S. Haque, P. Andrew, S. Hofmann, J. Moultrie, D. Chu, A. J. Flewitt, A. C. Ferrari, M. J. Kelly, J. Robertson, G. A. J. Amaratunga, W. I. Milne, *Proc. IEEE* **2012**, *100*, 1486.
[2] W. Cui, W. Lu, Y. Zhang, G. Lin, T. Wei, L. Jiang, *Colloids Surf. A* **2010**, *358*, 35.
[3] D. Ji, L. Jiang, Y. Guo, H. Dong, J. Wang, H. Chen, Q. Meng, X. Fu, G. Tian, D. Wu, G. Yu, Y. Liu, W. Hu, *Adv. Funct. Mater.* **2014**, *24*, 3783.
[4] R. Abargues, M. L. Martinez-Marco, P. J. Rodriguez-Canto, J. Marques-Hueso, J. P. Martinez-Pastor, *Adv. Resist Mater. Process. Technol. XXX* **2013**, *8682*, 86820X.

[5] J. Marques-Hueso, R. Abargues, J. Canet-Ferrer, J. L. Valdes, J. Martinez-Pastor, *Microelectron. Eng.* **2010**, *87*, 1147.
[6] J. Marques-Hueso, R. Abargues, J. L. Valdes, J. P. Martinez-Pastor, *J. Mater. Chem.* **2010**, *20*, 7436.
[7] J. A. Spechler, T.-W. Koh, J. T. Herb, B. P. Rand, C. B. Arnold, *Adv. Funct. Mater.* **2015**, *25*, 7428.
[8] D. S. Thompson, L. M. Davis, D. W. Thompson, R. E. Southward, *ACS Appl. Mater. Interfaces* **2009**, *1*, 1457.
[9] M. L. J. Liu, Y. Yang, L. Xu, J. Lin, W. Hong, X. Chen, *Adv. Funct. Mater.* **2017**, *27*, 1701674.
[10] K. Akamatsu, K. Nakahashi, S. Ikeda, H. Nawafune, *Eur. Phys. J. D* **2003**, *24*, 377.
[11] J. H.-G. Ng, D. E. G. Watson, J. Sigwarth, A. McCarthy, H. Suyal, D. P. Hand, T. Y. Hin, M. P. Y. Desmulliez, in *Proc. 36th Int. MATADOR Conf.* (Eds: S. Hinduja, L. Li), Springer London, London **2010**, p. 389.
[12] J. H. G. Ng, D. E. G. Watson, J. Sigwarth, A. McCarthy, K. A. Prior, D. P. Hand, Y. Weixing, R. W. Kay, L. Changqing, M. P. Y. Desmulliez, *IEEE Trans. Nanotechnol.* **2012**, *11*, 139.
[13] K. Akamatsu, S. Ikeda, H. Nawafune, H. Yanagimoto, *J. Am. Chem. Soc.* **2004**, *126*, 10822.
[14] K. Akamatsu, Y. Fukumoto, T. Taniyama, T. Tsuruoka, H. Yanagimoto, H. Nawafune, *Langmuir* **2011**, *27*, 11761.
[15] D. E. Watson, J. H. G. Ng, M. P. Y. Desmulliez, presented at 18th European Microelectronics & Packaging Conf., Brighton, UK, September **2011**.
[16] Y. Wang, N. Li, X. Wang, D. Havas, D. Li, G. Wu, *RSC Adv.* **2016**, *6*, 7582.
[17] A. V. Gaikwad, T. K. Rout, *J. Mater. Chem.* **2011**, *21*, 1234.
[18] H. W. Gerhard Naundorf, *US6319564*, **2001**.
[19] K. Akamatsu, S. Ikeda, H. Nawafune, *Langmuir* **2003**, *19*, 10366.
[20] J. Sharma, P. DiBona, D. A. Wiegand, *Appl. Surf. Sci.* **1982**, *11*, 420.
[21] M. Zhu, P. Chen, M. Liu, *J. Mater. Chem.* **2011**, *21*, 16413.
[22] L. W. Tilton, E. K. Plyler, R. E. Stephens, *J. Opt. Soc. Am.* **1950**, *40*, 540.
[23] a) R. Abargues, J. Marqués-Hueso, J. Canet-Ferrer, E. Pedrueza, J. L. Valdés, E. Jiménez, J. P. Martínez-Pastor, *Nanotechnology* **2008**, *19*, 355308; b) J. Marqués-Hueso, R. Abargues, J. Canet-Ferrer, S. Agouram, J. L. Valdés, J. P. Martínez-Pastor, *Langmuir* **2009**, *26*, 2825.
[24] K. A. Willets, R. P. V. Duyne, *Ann. Rev. Phys. Chem.* **2007**, *58*, 267.
[25] a) M. Xiao, R. Jiang, F. Wang, C. Fang, J. Wang, J. C. Yu, *J. Mater. Chem. A* **2013**, *1*, 5790; b) W. Hou, S. B. Cronin, *Adv. Funct. Mater.* **2013**, *23*, 1612.
[26] R. Abargues, K. Abderrafi, E. Pedrueza, R. Gradess, J. Marques-Hueso, J. L. Valdes, J. Martinez-Pastor, *New J. Chem.* **2009**, *33*, 1720.
[27] D. E. Watson, J. H. G. Ng, J. Sigwarth, J. Bates, M. P. Y. Desmulliez, *3rd Electronics System Integration Technology Conf. ESTC*, IEEE, Berlin, Germany **2010**.
[28] R. A. Farrer, C. N. LaFratta, L. Li, J. Praino, M. J. Naughton, B. E. A. Saleh, M. C. Teich, J. T. Fourkas, *J. Am. Chem. Soc.* **2005**, *128*, 1796.